J Mater Sci (2023) 58:14411–14425

Computation & theory

Does flute angle influence box performance?

Kelly Wade[1,*], Christine Todoroki[1], Aiman Jamsari[2], Eli Gray-Stuart[2], Stephen Tohill[3], John Bronlund[2], and Kate Parker[1]

[1] *Scion, Rotorua, New Zealand*
[2] *Massey University, Palmerston North, New Zealand*
[3] *Oji Fibre Solutions, Levin, New Zealand*

Received: 7 August 2023
Accepted: 8 September 2023
Published online: 23 September 2023

ABSTRACT

In the production of boxes, it is customary to align the flutes vertically, corresponding to a 0° flute angle. This configuration is widely believed to yield optimal compressive strength, despite existing evidence from corrugated flute boards and boxes that challenge this assumption. The present study investigates the hypothesis that non-vertical flute angles do not significantly compromise box compression strength and may potentially offer enhancements in other performance characteristics. Regular slotted container boxes (385 × 238 × 300 mm) constructed from single wall C-flute board were used in this study. Ten flute angles were selected for box level testing: 0°, 5°, 7.5°, 10°, 12.5°, 15°, 20°, 30°, 45° and 60°. Samples of converted board were subjected to edge crush testing (ECT) following TAPPI T-811 and four-point-bending following TAPPI T-820. Box crush testing (BCT) followed NZS 1301.800 2006 (New Zealand Standard). Component testing results were consistent with previous studies. Outcomes showed a general linear reduction in ECT with increasing flute angle, and nonlinear relationships between flute angle and bending force and stiffness. At the box level, peak load did not decline significantly between 0° and 45°, however 60° flute angles had significantly lower peak loads ($\alpha = 0.05$). At certain angles, notably 10° and 30°, less variation in peak load was observed. BCT force and stiffness of the box significantly improved in terms of median and variation at 10° and 30°. Therefore, a flute angle of less than 45° does not significantly reduce compression strength.

Introduction

Box production typically involves aligning flutes vertically with respect to the applied load, which is intuitively thought to offer maximum compressive strength. This is supported by experimental studies showing that boxes with vertically aligned flutes have 20% higher compression strength than horizontally aligned flutes [1] and corrugated board edge crush strength and bending force are generally highest in this direction [2–4]. Since boxes are themselves a hierarchical structure, the performance of

Handling Editor: Stephen Eichhorn.

Address correspondence to E-mail: Kelly.Wade@scionresearch.com

https://doi.org/10.1007/s10853-023-08941-2

the corrugated board will also depend on orientation of its component papers. In most vertical flute boxes, practical considerations dictate that the fibres of the component papers run perpendicular to the flutes due to the corrugating process. Therefore, the component papers are arranged directly opposite to the direction that they should be to provide maximum compressive strength in line with the flutes. Rotating the liners and medium by 90°, placing the fibres of the paper in line with the flutes (termed linear corrugating) improves both short and long-term box performance as the paper is better able to resist top-to-bottom loading and suffers less from hygro-expansivity [5].

While box performance is often quantified in terms of top-to-bottom crushing resistance, boxes experience multi-axial loading in service due to interactions with other boxes when palletised, interactions with the box contents and general shock and vibration through the supply chain. Both machine and cross direction properties of the component boards and papers have also been shown to play an important role in box performance [5–7]. The concept of optimising geometric means of the component paper performance has also been suggested as an avenue to maximise board performance [6].

Limited box-level studies have explored the performance of boxes whose components are not oriented either vertically or horizontally. Maltenfort examined the performance of fruit trays which were cut at a 45° angle in order to reduce wastage of board for the design in question. The fruit trays were unexpectedly found to have superior compression test performance compared to standard trays with vertically oriented flutes [8]. Curatalo examined the compressive strength of boxes for which flute angle ranged from 0° to 90° in 15° increments. Compression strength was found to increase nonlinearly as corrugations approached the vertical (i.e. closer to 0°) and parallel to the applied force, and concluded that end-to-end compression strength could be increased in a greater proportion than the corresponding reduction in top-to-bottom compression strength [7]. At the board level, Jamsari tested board samples (with angles 0°, 30°, 45°, 60°, 90°) in 4-point bending tests and found that the 30° and 45° samples improved bending stiffness compared to 0° without significantly affecting the maximum bending force [4]. As box performance is substantially influenced by panel bending, this finding suggests that angled flutes could bring performance benefits.

Recent investigations reveal further insights into component, board, and box behaviour. While McKee's approach is widely used industrially as it gives a simple, reasonable estimate of box, modern, more advanced techniques which account for aspect ratio and component properties give more accurate results. Such approaches have been reported as reducing error from between 8–15%, to around 6% [9]. This requires more detailed quantification of the orthotrophic strain in a material, as recently shown, an elegant method to achieve this involves use of ECT in both standard CD, but also at 45° in order to determine all strains for the material while monitoring with DIC (digital image correlation) and video extensometry [10]. A similar approach by the same authors involved creating a model to evaluate the compressive strength and stiffness of board in the CD, and validated this with experimental testing, monitored with DIC. This showed good agreement and that it was possible to use this to estimate the effects of changing different layers within the board. It also showed the importance of using optical strain measurement given the inherent compliance in test machine crossheads [11]. An analytical study of bending stiffness of five-layer corrugated board based on paper properties and board geometry showed that liners contributed almost all the bending stiffness of the board, at least in MD, where the fluting medium contributed less than 1% to the overall bending stiffness of the board. For asymmetric board, the orientation of the board during testing influenced the bending stiffness, as would be expected. Similarly, alterations to liner thickness or defects greatly influenced the board performance [12]. A modelling and numerical homogenisation approach exploring effects of grammage on ECT and BCT showed paper configuration is important. The influence of grammage changes depends on board asymmetry; changing the heaviest liner had the largest effect, and increasing fluting weight reduces the sensitivity to liner variation [13]. A simplified modelling approach for ECT of multi-layered board, included tensile testing of paper at 45° to generate validation data for the analytical models [14]. A machine learning approach to estimate ECT based on paper and board characteristics appeared promising and included training data which accounted for loading at different angles. Interestingly, the different flute profiles in the training data had different proportional changes in ECT as flute angle changed [15]. Other recent studies emphasise the importance of reducing variability in the data any

estimates of box and board performance are based on, be this paper properties, ECT or BCT [16, 17].

Considering the practical difficulties of rotating paper components at industrial scale, this investigation will explore possible strategies to improve box performance within the constraints of standard corrugated board as a source material. One option is to rotate the board itself during die cutting and create boxes with angled flutes. Vertical flutes were defined as 0° flute angle and horizontal flutes as 90° flute angle. We tested the hypothesis that non-vertical flute angles do not significantly reduce box compression strength and may in fact confer advantages in other aspects of performance. Our goal was to confirm these phenomena at the box level using mechanical testing in order to provide data to inform subsequent modelling or experimental investigations. Considering that the studies referenced above use relatively large incremental angles (i.e. 15°, or 30°), we evaluated 10 flute angles that ranged from 0° to 60°, mainly concentrated within 0 to 20° in order to gain insights which may not have been captured previously. We conducted box crush testing (BCT) at each flute angle, along with edge crush testing (ECT), and four-point bending of the component board.

Materials and methods

Regular slotted container (RSC) boxes (385 × 238 × 300 mm) were used in this study, constructed from single wall C-flute board (200 gsm Kraft linerboards with 150 gsm semi-chemical medium) supplied by a New Zealand papermaker. The geometric characteristics of the board are given in Table 1 and the details of each paper component are listed in Table 2.

Ten flute angles were selected for box level testing: 0°, 5°, 7.5°, 10°, 12.5°, 15°, 20°, 30°, 45° and 60°. These boxes were created using a cutting table (Zünd) and were stored in a dry environment in a flat packed state to prevent damage prior to testing. They were assembled using standard brown packing tape to hold top and bottom flaps in place.

Table 1 Geometric characteristics of corrugated board used in this research

Board thickness (mm)	3.90
Flute height (mm)	3.39
Flute pitch (mm)	7.67
Take-up factor	1.43

Table 2 Properties of the constituent paper that made up the board

Paper	Inner	Flute	Outer
Thickness (mm)	0.253	0.204	0.253
Grammage	205	163	205
Density (kg m^{-3})	791	784	791

Component testing was conducted in parallel with the box crush testing in order to enable comparison of predicted BCT via the McKee equation (Eq. 1) [18] with experimentally measured BCT. This testing followed the procedure described by Jamsari [4] involving edge crush testing (ECT) and four-point bending testing in the machine direction (MD) and cross direction (CD). Three box blanks of each angle were reserved for ECT and four-point-bending, and broadly equal numbers of samples were cut from these to distribute variation equally during testing. Samples were cut from box blanks in order to test material most representative of the boxes themselves; sampling locations were chosen to exclude any of the creased or regions close to the creased areas. Following cutting, samples were stored in controlled conditions at 23 °C at 11% RH for at least 48 h and then 50% RH for at least 24 h prior to testing in accordance with the TAPPI T-402 standard. At least ten ECT, vertical, and horizonal four-point bending samples were tested at each flute angle.

Theoretical BCT calculation

The component property results were also used in the McKee equation [18] as a comparison with experimental data.

$$\mathrm{BCT} = 2.028\mathrm{ECT}^{0.746}\left\{\sqrt{\left(D_{\mathrm{MD}}D_{\mathrm{CD}}\right)}\right\}^{0.254}Z^{0.492} \quad (1)$$

where BCT and ECT are the box and edge crush forces (in N), D_{MD} and D_{CD} are, respectively, the machine direction and cross direction stiffnesses (N m), and Z is the perimeter of the box which is 1.24 m in the current study.

Edge crush test (ECT)

Samples for ECT were cut from converted board panels using an Epilog Fusion M2 laser cutter into

38.1 × 50.8 mm rectangles following the TAPPI T-811 standard (Fig. 1). Samples were cut at each flute angle (relative to the vertical edges of the box) referred to above. Approximately 6 mm from each end of the sample was reinforced with paraffin wax prior to conditioning to prevent failure in these regions during testing.

The experiment was run using a texture analyser (TA.XT Plus, Texture Technologies Corp.) with a constant displacement speed of 12.5 mm min^{-1}. At the start of each test, two metal blocks were used as guides to ensure that the sample was held vertically. These were manually removed when the force was between 22 and 67 N as indicated in TAPPI T-811 standard. ECT force was calculated by dividing maximum force by sample width, (50.8 mm). Typical force–displacement curves for ECT are shown above in Fig. 2.

Four-point bending

Samples for four-point bending (260 × 50.8 mm samples in accordance with TAPPI T-820) were cut from converted box panels using the laser cutter. Samples for bending tests were cut relative to the vertical and horizontal edges of the box for each of the 10 flute angles, Fig. 1. As with ECT, the texture analyser was used to apply a constant displacement speed of 12.5 mm min^{-1} to the samples. The centre deflection of the sample during the test was measured using a laser displacement sensor. Following testing, a graph of force against centre deflection was plotted for each trial and the bending stiffness calculated using Eq. 2:

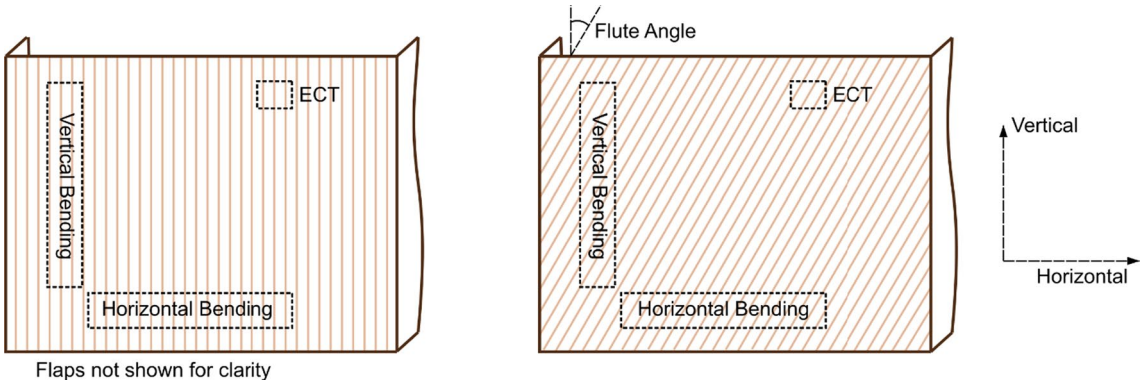

Figure 1 Example box panels showing how flute angle is defined relative to the box edges in this investigation and how this relates to the ECT and vertical or horizontal four-point bending samples.

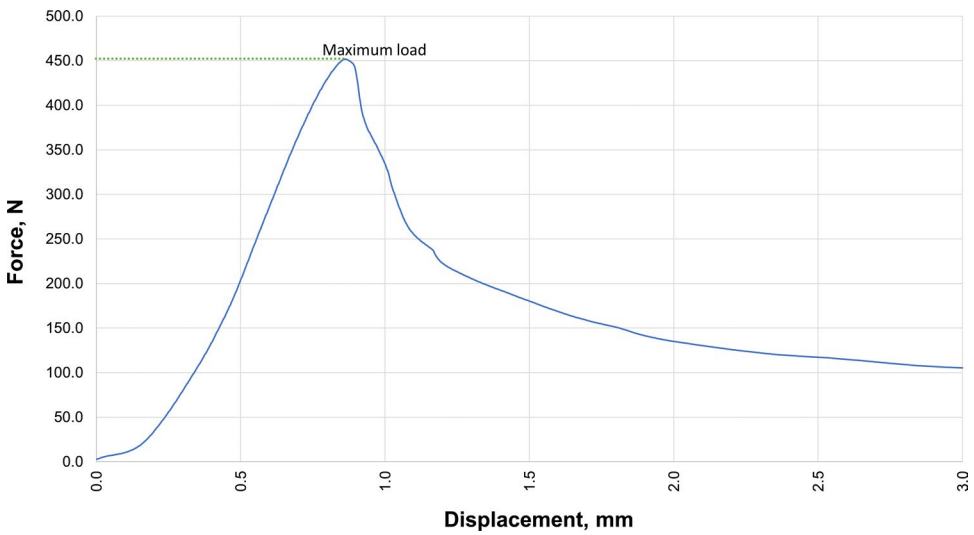

Figure 2 Typical force–displacement curves for ECT of board at a 0° flute angle. Maximum load was determined for each curve as indicated by the green line.

$$D = \left(\frac{1}{16}\right)(\Delta)\left(\frac{L_{\text{bottom}}^3}{w}\right)\left(\frac{a}{L_{\text{bottom}}}\right) \quad (2)$$

where D is the flexural stiffness (N m), Δ is the slope of the force against centre deflection graph (N m^{-1}), L_{bottom} is the distance between both the bottom anvils (m), w is the width of the sample (m) and a is the distance between the bottom and upper anvil (m) at either end.

Sample performance was assessed in terms of peak bending force and bending stiffness. Typical force–displacement curves for bending stiffness tests are shown above in Fig. 3.

Box crush testing (BCT)

Boxes were tested according to NZS 1301.800 2006 (New Zealand Standard) [19]. Ten boxes (the recommended minimum number of samples for this standard) of each flute angle were used in the present study to maximise the number of flute angles that could be tested. The boxes were conditioned for 48 h at 23 °C and 50% RH to ensure consistent equilibrium moisture content prior to testing. A Wiedemann 60CS universal tester fitted with fixed platens was used to compress boxes at a crosshead speed of 10 mm min^{-1} until failure.

As shown in Fig. 4, the highest load prior to failure was recorded as the BCT load (also known as the load

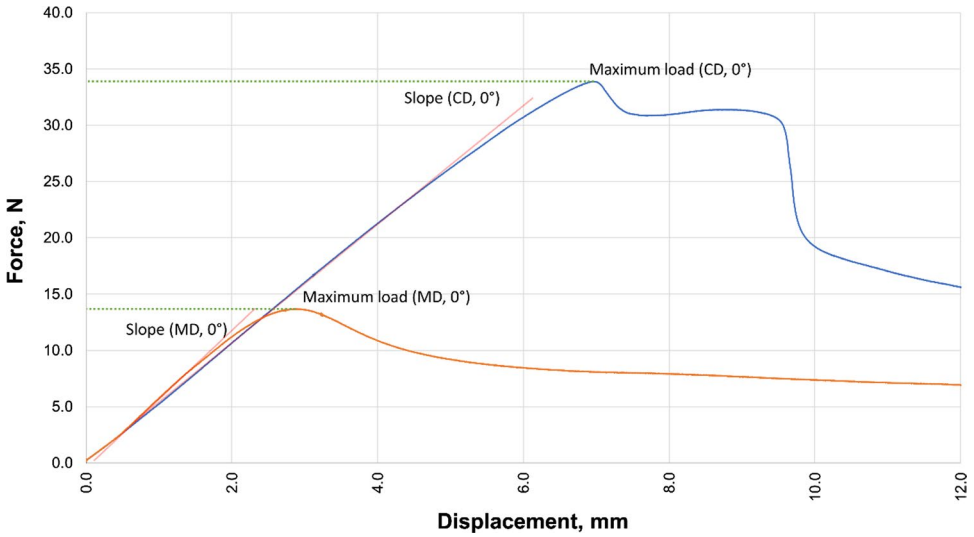

Figure 3 Typical force–displacement curves for four point bending of board at a 0° flute angle in the CD (blue) and MD (red). Slope and maximum load was determined for each curve as indicated by the red and green lines, respectively.

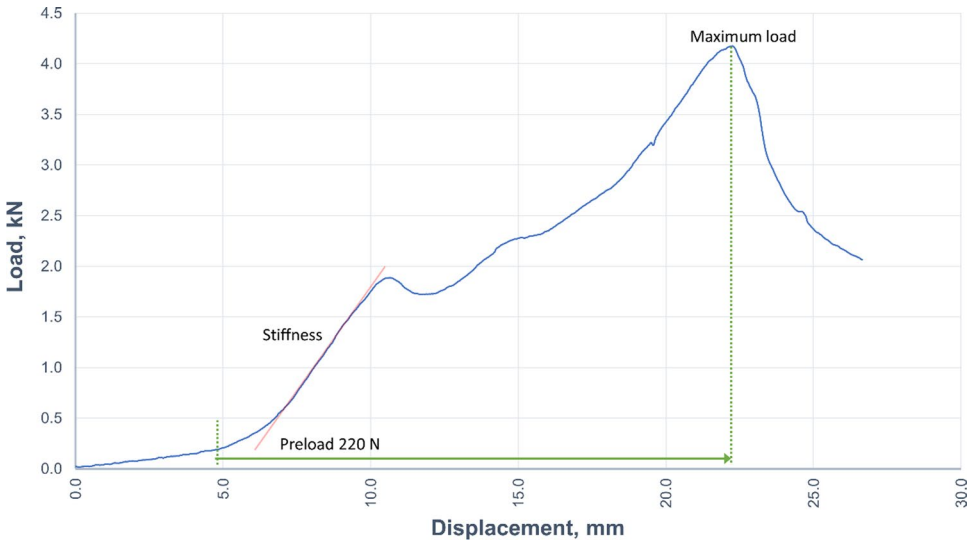

Figure 4 A typical load–displacement curve (shown in blue) for boxes similar to those used in the present study. Maximum load (green dashed line), displacement at maximum load and stiffness (red line) were determined from these curves, along with the preload of 220 N (region covered by green arrow).

to failure—LTF). Displacement was measured from a preload of 220 N as specified in the standard. The boxes exhibited a discontinuity in their load displacement curve at approximately 1.8 kN of loading. Our observation from testing of similar boxes indicated this was due to crushing of the flap creases, in addition to the preliminary low stiffness region where the flaps themselves are compressed as noted in previous studies [20, 21]. Garbowski et al. have reported that this discontinuity is a consequence of offset between the horizontal crease lines causing the upper part of the creased material to contact the platen first [22]. This discontinuity was not related to buckling of the box panels themselves. In the present study, we focussed on analysing the stiffness of the first linear region after compression of the flaps as the magnitude of loading in this region is closest to the loading the boxes would experience in service.

Statistical analysis

All analyses were conducted using R Version 4.2.1 [23], supplemented by packages 'plyr' [24], and 'PMCMRPlus' [25]. To determine if flute angle significantly affected the response variables (Force, or Stiffness) the Kruskal–Wallis rank sum test was applied [26]. This nonparametric test was used in favour of parametric models and ANOVA analyses, following Lantz [27], because sample distributions were not normally distributed. Normality was tested using the Shapiro–Wilk test [28] and homogeneity of variances was tested using the Fligner-Killeen test [29]. Therefore, the Kruskal–Wallis test, which makes no assumptions about the underlying distributions was appropriate. When the Kruskal–Wallis rank sum test indicated significant differences ($\alpha = 0.05$), post-hoc testing via Dunn's many-to-one comparison test (i.e. pairwise comparisons of flute angles with the 0° control) [30] was invoked, using a two-sided alternative hypothesis, to determine which flute angles differed significantly to the control. Though our focus was on those comparisons for which $p < 0.05$, we note that p-values represent only an index to evidence [31] and do not imply practical significance [32]. Therefore, we also considered results for which p exceeded 0.05 but was less than 0.10. Statistical comparisons were supplemented with visual analyses using box-and-whisker plots (see Figs. 3 and 5 for details).

To examine overall trends in relationships between flute angle and maximum force (for both ECT and BCT trials), linear and second-order polynomial models were evaluated with flute angle as the explanatory variable and force as the response. The best models were selected following comparisons using ANOVA, and 95% confidence and prediction intervals calculated over the range of flute angles.

In addition to testing for statistically significant differences between flute angles and force, or stiffness, a system was developed to determine which angle performed best overall in terms of having both the greatest values (on average) and the least variation. Average was assessed in terms of median values and variation assessed using median absolute deviation (MAD). Median and MAD statistics were chosen in favour of mean and standard deviation, primarily due to non-normality and small sample sizes. Following concepts derived from data envelopment analyses [33–35], to essentially rank what are known as "decision making units" (our DMUs here are the flute angles), we plotted median and MAD values at each angle, then calculated the Euclidean distance from each point to an "ideal" point having maximum magnitude (i.e. the greatest median) and no variation (i.e. MAD is equivalent to zero). Following López-Espín et al. [36] who argued that "the distance to the efficient projection point should be minimised", we determined the angle of best performance.

Results

The principal discovery of this study was that the box crush testing (BCT) performance, or load-bearing capacity, exhibited relative consistency when the flute angle ranged from 0° to approximately 30°. This observation is evident in the summary statistics of the trials, as presented in Table 3. A noticeable decline in performance at a 60° flute angle is apparent across all trials and both measured attributes (force and stiffness). Nevertheless, the variation at 60°, as evaluated by the standard deviation (sd), was generally smaller than the variation associated with other flute angles.

Component testing

The component test results and their relationship to BCT performance are summarised in Fig. 5. Figure 5a shows a general linear reduction in ECT strength with increasing flute angle, consistent with other studies of how ECT relates to flute angle [2, 4]. The linear

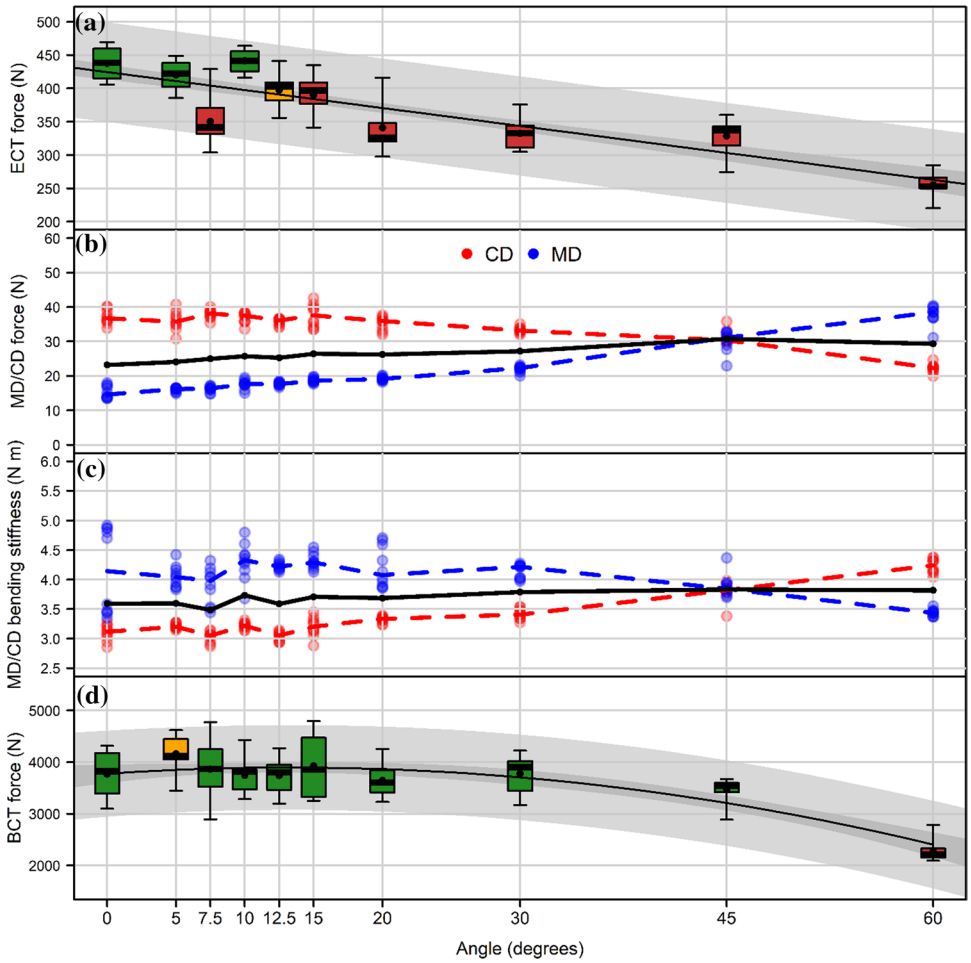

Figure 5 Box and whisker plots depicting maximum force for: ECT trials (**a**) and vertical and horizontal trials (**b**), bending stiffness for vertical and horizontal trials (**c**), and maximum force for BCT trials (**d**). Flute angles that do not differ significantly to 0° are shown in green, those for which $p < 0.05$ in red, and those for which $0.05 < p < 0.10$ in orange. Vertical and horizontal bending test results are shown in red and blue, respectively, and combined results in black. Shaded areas depict 95% confidence intervals (inner regions) and 95% prediction intervals (outer regions). Estimated mean BCT force values using McKee's equation are shown as asterisks, with line segments representing one standard deviation.

Table 3 Summary statistics (mean ± sd) for the box crush and bending test trials

Flute angle (°)	ECT force (N)	MD force (N)	MD stiffness (N m)	CD force (N)	CD stiffness (N m)	BCT force (N)
0	438 ± 23	15.3 ± 1.8	4.1 ± 0.7	37.2 ± 2.1	3.1 ± 0.1	3768 ± 439
5	420 ± 23	16.0 ± 0.6	4.1 ± 0.2	36.0 ± 2.8	3.2 ± 0.1	4160 ± 341
7.5	350 ± 37	16.2 ± 0.8	3.9 ± 0.3	38.0 ± 1.3	3.0 ± 0.1	3865 ± 569
10	442 ± 17	17.6 ± 1.3	4.3 ± 0.3	36.9 ± 1.6	3.2 ± 0.1	3745 ± 326
12.5	397 ± 27	17.7 ± 0.5	4.2 ± 0.1	35.8 ± 0.9	3.0 ± 0.1	3741 ± 325
15	390 ± 30	18.7 ± 0.7	4.3 ± 0.1	37.5 ± 3.3	3.2 ± 0.2	3926 ± 586
20	341 ± 40	19.2 ± 0.6	4.2 ± 0.3	35.3 ± 1.9	3.3 ± 0.1	3644 ± 319
30	332 ± 22	22.0 ± 0.9	4.1 ± 0.1	33.4 ± 0.9	3.4 ± 0.1	3774 ± 348
45	329 ± 26	30.2 ± 3.0	3.9 ± 0.2	31.1 ± 1.9	3.8 ± 0.2	3469 ± 229
60	255 ± 16	37.8 ± 2.7	3.4 ± 0.1	22.2 ± 1.2	4.2 ± 0.1	2270 ± 197

model had an intercept of 424.6 N, and gradient of − 2.7 N degree^{-1} (Table 4) indicating that for each unit increase in flute angle, estimated force declined by 2.7 N. The model explained about 63% of the variance (R^2 adj = 0.63).

Four point bending results, summarised in Fig. 5(b, c) were also consistent with the literature [4], showing a nonlinear change in terms of force or bending stiffness with flute angle, and a crossover in properties at 45° as would be expected. Note that the 0° to 10° MD

Table 4 Results of the regression analysis for estimating ECT Force from flute angle

Coefficients	Estimate	Std. error	p-value
Intercept	424.6	5.7	< 2e−16
Angle	− 2.7	0.2	< 2e−16
Residual standard error: 37.25 on 96 degrees of freedom			
Multiple R-squared: 0.6384, Adjusted R-squared: 0.6347			

results showed more variation than the other angles. At these angles, it is important to ensure that the flute tips meet the point on both bottom anvils before conducting the test as explained in TAPPI T 820. However, for some samples, as the loading started, the samples slightly moved as a result of inertia, hence the larger deviation seen in these angles as opposed to others. Overall bending stiffness of the panel from the combined vertical and horizontal bending tests is shown by the black line in Fig. 5c. This shows that there was a localised peak in bending properties at 10° and combined properties appeared to maximise at 45° but was also higher than 0° at 30° and 60°. In particular, as shown in Fig. 5c, there was a clear local peak of combined bending stiffness at 10°.

Experimental and theoretical BCT results

Figure 5d shows both the experimental BCT results and theoretical values calculated based on component testing results. There was no significant difference in experimentally measured BCT from 0° to 30° and the predicted BCT followed a similar trend. While experimental values were higher than those estimated using McKee's equation, the difference between the two was also not significant. This could be a consequence of the McKee equation coefficients not matching this situation perfectly.

Box failure morphologies

There were clear differences in the failure morphologies of each box. The linerboards appeared to cockle (or wrinkle), until the panel buckled at peak load and creases travelled across the box panel with subsequent compression. As shown in Fig. 6, the creases followed the flutes once the box buckled, although in most cases these creases travelled inwards from the corners of each box to a central parallelogram panel as observed in previous studies. An exception was the 60° box group, in which creases travelled across the whole panel and the failure load was significantly lower ($p < 0.001$). Most of the boxes (all but 60°) exhibited the typical loading curve expected for RSC boxes (Fig. 2) with a discontinuity at approximately 2.3 kN. As mentioned in the Methods, this was related to compression adjacent to the flap creases for boxes made on the cutting table, not due to failure of the panels themselves. No significant relationships were observed in terms of whether flute angle could have influenced the point at which these creases compressed or the behaviour of the box before or after the discontinuity. Consequently, analysis focussed on the maximum force, and the stiffness of the loading curve prior to the discontinuity (hence simply referred to as stiffness), as these properties are relevant to loading of the box and all showed significant variation as the flute angle was changed.

Influence of flute angle on box stiffness and displacement at failure

As can be seen in the summary of BCT results in Fig. 7, there were no significant differences in peak forces between vertical flutes or any of the flute angles from 5° to 45°. Force was greatest at 5° followed closely by 30° and 7.5°. Only 60° boxes were significantly lower (as shown in Table 5, $p < 0.001$). In terms of stiffness, both 30° and 10° boxes exhibited significantly higher values ($p < 0.001$) than the other groups, including the 0° boxes. Again, 60° boxes had a significantly lower stiffness than vertical flute boxes.

There were significant differences in displacement at failure between the 0° boxes and the 7.5°, 10°, 12.5°, 15°, 20° and 60° boxes. In all these cases, the displacement at failure was significantly lower than for the vertical flute boxes. As shown in Fig. 7, the magnitude of this difference was around 2 mm.

In terms of both magnitude and variation as summarised by the MAD diagrams in Fig. 8, 5° demonstrated the best performance for force, followed by 10° and 30°. For stiffness the best performance was for 30°, followed by 10° and 45°. 60° boxes had the poorest performance in terms of both parameters.

Discussion

In general, these findings are consistent with previous experimental studies at both the board and box levels, which have indicated that compressive performance

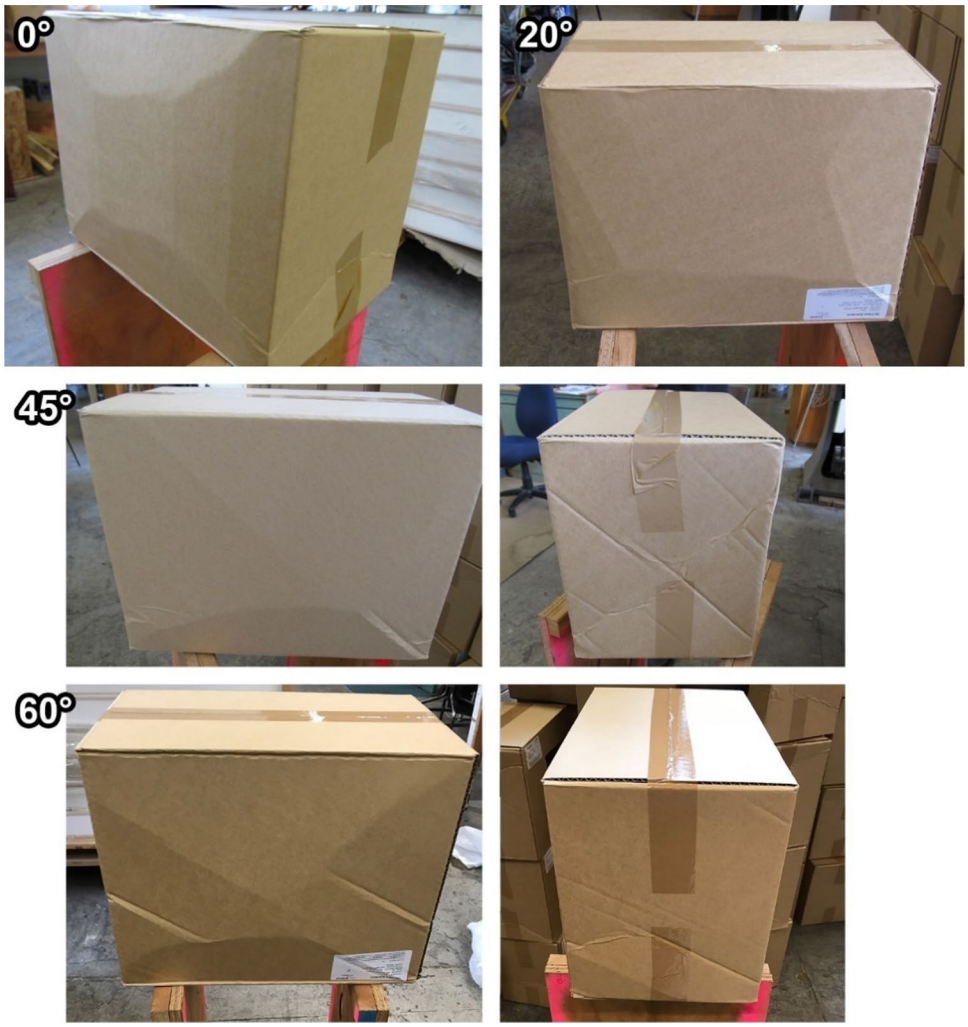

Figure 6 Failure morphologies of boxes following BCT testing. Creasing of each panel is clearly visible. Note that the creases travel across the whole panel in the cases where no complete flutes connect the upper and lower panel edges (short end of 45° and both the long and short faces of the 60° box).

should not decrease rapidly or linearly with variations in flute angle [4, 7, 8]. By testing a close range of angles between 0° and 20°, the present study provides experimental data not available previously. In contrast to the maximum load-bearing capacity of the box, the stiffness of the box did show significant variation across the tested range of flute angles. The local peaks for combined MD and CD stiffness at 10° and higher values at 30° (Fig. 5c) are consistent with the peaks in overall box stiffness measured experimentally (Fig. 7b) and the concept of the MD and CD stiffness of the board governing panel buckling and playing an important role in the overall performance of the box [4, 6, 18, 37]. While the geometric mean of the board stiffness (Fig. 5c, black line) was highest at 45°, this does not correspond to the box level results. This is likely a consequence of the box geometry: at 45° the short side panels no longer contain complete flutes from corner to corner, and these panels buckled readily with creases spanning the whole panel as can be seen in the examples in Fig. 6. Thus, it is reasonable to conclude that these panels were unable to contribute fully to the overall box stiffness. Likewise, in the case of the 60° scenario, where this behaviour was observed for all panels, both the failure load and the stiffness were significantly lower.

There were also significant differences in displacement at failure (Fig. 7c). Since the present study measured the overall displacement of the box, it was not possible to distinguish whether this difference was due to differences in behaviour of the panels or the creases. This could be a topic for subsequent studies, given that it has been shown that a substantial portion (approximately half) of box vertical displacement is related to displacement of the creases [21]. The magnitude of this difference was approximately 2 mm

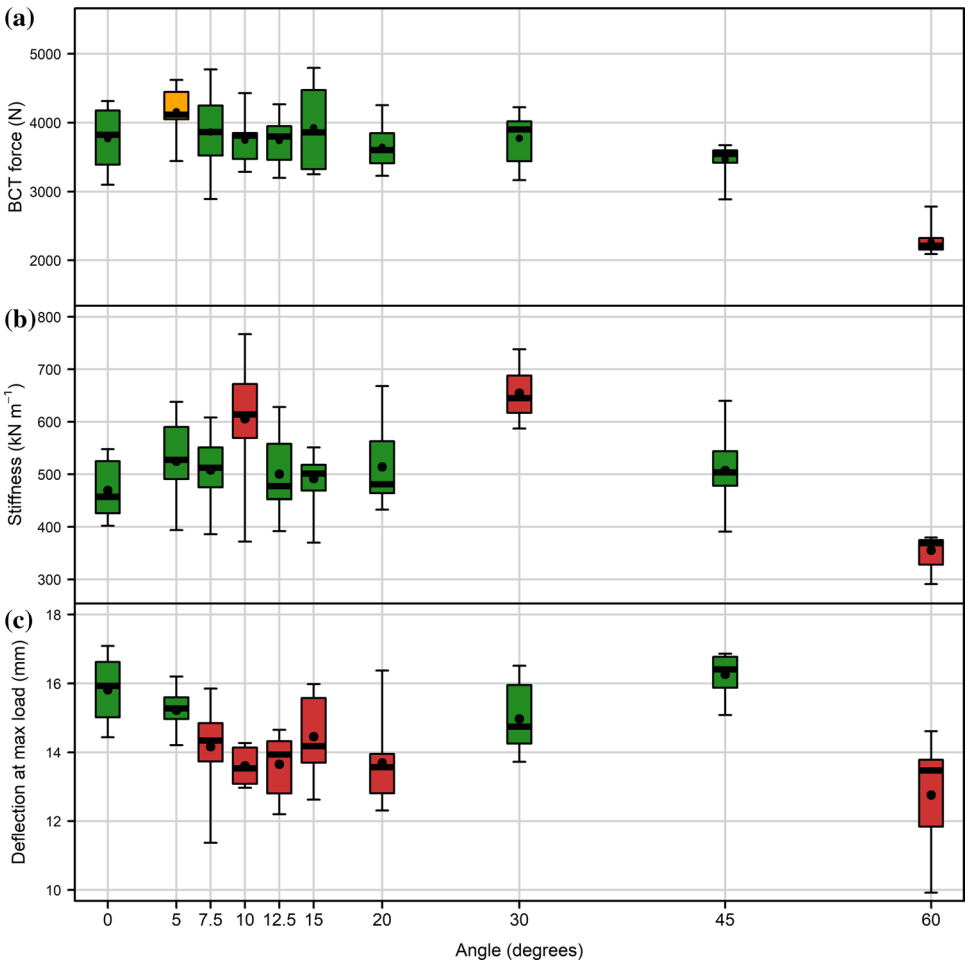

Figure 7 Data distributions of BCT trials: force (top panel), work (middle panel), stiffness, and deflection (bottom panel). Boxes shown in green are not significantly different to the 0-degree distributions, red indicates significant difference at $\alpha = 0.05$. Median values are indicated by horizontal lines, means by black dots, and outliers by asterisks.

Table 5 Summary of *p*-values resulting from pairwise comparisons between flute angle and the control (post-hoc Dunn tests) on BCT data

Variable	0–5	0–7.5	0–10	0–12.5	0–15	0–20	0–30	0–45	0–60
Max load	0.061								< 0.001
Displacement at maximum load		0.009	< 0.001	< 0.001	0.018	< 0.001			< 0.001
Stiffness			0.003				< 0.001		0.019

which, though not substantial in terms of the overall height of the box, could be relevant to the end use of the box; these boxes had a typical headspace of 10 mm. As above, this behaviour depends on both panel and crease properties. The distance between flutes will increase as flute angle increases and this may influence the way the crease behaves under compression.

This raises the question: Why might these improvements and differences in performance occur at certain angles? Natural hierarchical structures including wood, bone and connective tissues contain numerous examples of anisotropy. Subsequent to conducting the experimental work for the present study we became aware of the concept of the magic angle. This describes the maximum enclosed volume for a helical reinforcing fibre of fixed length in a cylinder, but is also valid for a flat sheet reinforced by fibres in the plane. This angle, 35.26° and its complement, 54.74° was initially identified in nemertean worms [38], but as the name suggests, appears as if by magic in numerous diverse settings [39, 40]. It is similar to the fibre angle of the intervertebral disc [41], arteries [42], and the spiral angle observed in certain trees [43]. Industrially, it is known to reduce the tendency of hoses to distort when

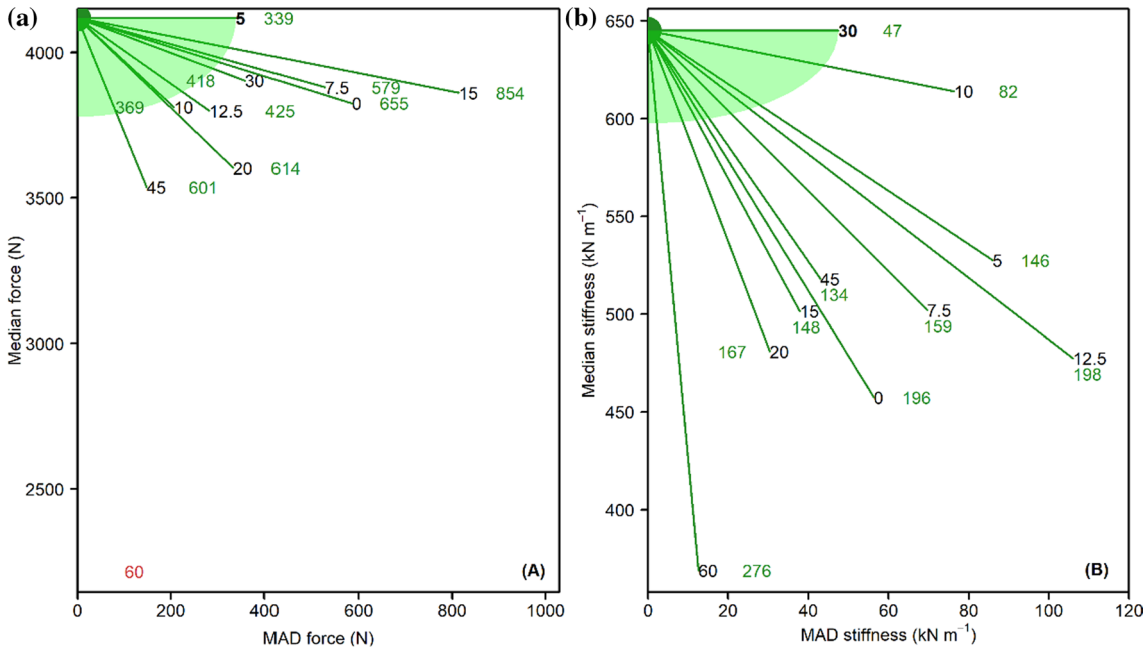

Figure 8 Performance of angles in BCT trials assessed using mean force (**a**), or median stiffness (**b**), and variation (MAD) to determine distance (shown in green font) from a hypothetical 'ideal' point (green point at top left). Flute angles with the best performance (i.e. shortest distance) are indicated in bold black font. Red font indicates that median force of the 60° flute angle was significantly lower than the control (0°) and therefore distance was excluded.

pressurised [44]. If the flutes of a box are arranged at one of these angles (35.26° or 54.74°), the component papers in that board will be at the other. Considering this, the increase in stiffness observed in the 30° boxes could be a consequence of their constituent papers and flutes approaching this angle.

Note also that the S2 layer of the plant cell wall which plays an important role in the stiffness of wood typically varies between 5° and 20° [45–48], although other angles are possible [49]. While generally a steeper angle is considered to result in a stiffer structure, intuitively situation specific differences in aspect ratio and material properties would be expected to influence this, which could explain the finding of the present study that 10° appears to result in optimal stiffness.

These observations could have implications for how such boxes would perform in service. Since variability in BCT is considered to be linked to variability in creep performance [50], the potential of angle flutes to reduce variability in lifetime should also be considered. Similarly, while links between BCT performance and lifetime are well established, the influence of box stiffness on creep performance could also be worthy of consideration. Increased stiffness due to variation in microfibril angle has been linked to reduction in creep rate for wood samples [51–53] which could be analogous to the component orientation in this situation. The increased stiffness observed for angle flutes boxes at 10° and 30° would be relevant to the loading levels the boxes would be subjected to in service, and the corresponding reduction in deflection for a given load would intuitively appear to be likely to reduce susceptibility to creep. Given the role of hygroexpansive stress in accelerated creep performance of boxes [5, 50], it could be speculated that angle flute boxes may deform preferentially (in a direction governed by the flute angle) as a result of creep. If true, this could prove advantageous in palletization—boxes could be arranged to form pallets which self-reinforce as a consequence of creep loading. Altering the flute angle of the box panels may also improve the response of the box as it interacts with its contents, known to play a substantial role in long-term storage performance of the box [54]; this is also a factor that should be considered in future investigations.

Creating boxes with 30° angled flutes is likely impractical for the regular slotted containers used in the present study, which are cut as vertical strips. Nonetheless, as mentioned in the Introduction, the

performance gains related to increased stiffness and reduced variability may prove to outweigh the proportion of board that is wasted. For more irregular shapes such as fruit trays, cutting boxes at an angle has been shown to be a strategy to save board as it is possible to interlock the blanks and reduce board use [8]. The potential to cut angled flute inserts to strategically reinforce boxes may also be worth considering.

Another motivation behind this study was to investigate the possibility of cutting blanks at an angle to reduce die shock during cutting. This occurs when a cutter blade strikes parallel to a glue line, resulting in increased tool wear and energy use. Intuitively, this is much less likely to occur if blanks are being cut at an angle. While assembling the boxes, it was notable that folding the angle creases required more care than for vertical boxes to avoid unintended folding of the blank parallel to the flute. Although this was a qualitative observation, it is a factor that would require consideration if this strategy were to be implemented.

While not considered in the present study, board crushing due to printing and conversion could potentially influence performance of angle flute boxes. It is known that this can influence the performance of single and double-walled board, with lower levels, below 30% being approximately linear [55, 56]. More severe crushing can cause delamination of the flute [4]. Conversely a study on board post conversion indicated that differences pre- and post-conversion were insignificant [57]. Given that crushing influences the medium and glue joints, it is likely that this could act at a different magnitude to that observed in vertical flute boxes, but this would need to be confirmed experimentally. For example, during printing using rotary dies the forces would be balanced across larger distances (flute tip to flute tip) in angle flute boxes.

The present results clearly show that altering the flute angle does not significantly reduce the short-term load bearing ability of the box over a wide range of angles, between 0 and 45° from vertical. As could be surmised from relationships such as the McKee equation, this is likely a result of synergy between crush strength and bending stiffness. There were significant effects on the stiffness of the box, particularly at 10° and 30°, and in the case of stiffness, there is reason to hypothesise that this could improve the long-term stacking (creep) performance of the box. Another potential benefit is that increased stiffness in the horizontal direction will assist preventing bowing of the panel associated with hydrostatic loading imposed by the product in the box.

Conclusions

This study investigated the influence of flute angle on box compression strength and response to loading. Box crush test performance in terms of force alone did not significantly reduce when flute angle was varied between 0° and 45°. Some angles had higher mean forces, and many angles tested (notably 10° and 30°) showed substantially less variation in peak load. Stiffness showed substantial and significant improvements at certain flute angles compared to 0°. Both 10° and 30° had significantly higher stiffness and lower variation in their performance. Component board properties were also tested and indicate that while ECT reduces almost linearly with flute angle, bending performance does not, consistent with literature and the concept that overall box performance depends on these component properties. These results suggest that varying flute angles of boxes to reduce die shock and/or to optimise board use is unlikely to significantly reduce box performance, at least for the RSC boxes used in the present study. Conversely, varying the flute angle may bring performance benefits by increasing box stiffness and reducing variation in performance.

Acknowledgements

We would like to thank Bruce Davy, Donna Smith, Robin Parr and Garth Weinberg for their assistance in conducting the box crush testing. We would like to thank Alan Dickson, Michelle Sloane and Alec Foster for their support in reviewing the final manuscript. We would also like to thank Oji Fibre Solutions for supplying the boxes used in this study.

Authors' contributions

All authors were involved in initial conceptualisation of the study. KW supervised the box level testing and drafted the initial manuscript. CT conducted statistical analysis of the data from all testing. AJ and EG conducted component level testing. All authors reviewed the manuscript.

Funding

Open Access funding enabled and organized by CAUL and its Member Institutions. Funding for this work was provided by Ministry for Business, Innovation and Employment (NZ) via the Strategic Science Investment Fund, Grant 79192.

Availability of data and materials

Underlying data (mechanical test load–displacement values and images) are available upon request.

Declarations

Conflict of interest The authors have no competing interests to declare that are relevant to the content of this article.

Ethical approval and consent to participate Not applicable; this research did not involve people or animals.

Consent for publication All authors agree with the content of this manuscript and consent to its publication.

Supplementary Information The online version contains supplementary material available at https://doi.org/10.1007/s10853-023-08941-2.

References

[1] Panyarjun O, Burgess G (2001) Prediction of bending strength of long corrugated boxes. Packag Technol Sci Int J 14(2):49–53

[2] McLain TE, Boitnott RL (1982) Crush tests rely on parallel-to-flute loading. Tappi J 65(3):148–148

[3] Lee MH, Park JM (2004) Flexural stiffness of selected corrugated structures. Packag Technol Sci Int J 17(5):275–286

[4] Jamsari MA et al (2019) Experimental and numerical performance of corrugated fibreboard at different orientations under four-point bending test. Packag Technol Sci 32(11):555–565

[5] Popil RE, Hojjatie B (2010) Effects of component and orientation on corrugated container endurance. Packag Technol Sci 23:189–202

[6] Urbanik TJ (1996) Machine direction strength theory of corrugated fiberboard. J Compos Tech Res 18(2):80–88

[7] Curatalo R (2000) A Comparative study of the compression strength of corrugated shipping containers and corrugated board, based on different corrugation directions

[8] Maltenfort GG (1988) Corrugated shipping containers: an engineering approach. Jelmar Publishing Co., Plainview

[9] Garbowski T, Gajewski T, Grabski JK (2020) The role of buckling in the estimation of compressive strength of corrugated cardboard boxes. Materials 13(20):4578

[10] Garbowski T, Knitter-Piątkowska A, Marek A (2021) New edge crush test configuration enhanced with full-field strain measurements. Materials 14(19):5768

[11] Garbowski T, Grabski JK, Marek A (2021) Full-field measurements in the edge crush test of a corrugated board—analytical and numerical predictive models. Materials 14(11):2840

[12] Garbowski T, Knitter-Piątkowska A (2022) Analytical determination of the bending stiffness of a five-layer corrugated cardboard with imperfections. Materials 15(2):663

[13] Mrówczyński D, Knitter-Piątkowska A, Garbowski T (2022) Non-local sensitivity analysis and numerical homogenization in optimal design of single-wall corrugated board packaging. Materials 15(3):720

[14] Garbowski T, Knitter-Piątkowska A, Winiarski P (2023) Simplified modelling of the edge crush resistance of multilayered corrugated board: experimental and computational study. Materials 16(1):458

[15] Garbowski T, Knitter-Piątkowska A, Grabski JK (2023) Estimation of the edge crush resistance of corrugated board using artificial intelligence. Materials 16(4):1631

[16] Frank B, Cash D (2022) Edge crush testing methods and box compression modeling. Tappi J 21:418

[17] Frank B, Kruger K (2021) Assessing variation in package modeling. Tappi J 20(4):231–238
[18] McKee RC, Gander JW, Wachuta JR (1963) Compression strength formula for corrugated boxes. Paperboard Packag 48(8):149–159
[19] AS/NZS 1301.800S-2019 Methods of test for pulp and paper—Compression resistance of fibreboard boxes (cases). 2019, Standards New Zealand
[20] Frank B (2014) Corrugated box compression - a literature survey. Packag Technol Sci 27:105–128
[21] Kueh CSL et al (2019) Digital image correlation analysis of vertical strain for corrugated fiberboard box panel in compression. Packag Technol Sci 32(3):133–141
[22] Garbowski T, Gajewski T, Knitter-Piątkowska A (2022) Influence of analog and digital crease lines on mechanical parameters of corrugated board and packaging. Sensors 22(13):4800
[23] R Core Team (2022) R A language and environment for statistical computing. R Foundation for Statistical Computing, Vienna
[24] Wickham H (2011) The split-apply-combine strategy for data. Analysis 40(1):1–20
[25] Pohlert T (2022) Calculate pairwise multiple comparisons of mean rank sums extended
[26] Hollander M, Wolfe DA (1973) Nonparametric statistical methods, vol 751. Wiley, Hoboken
[27] Lantz B (2013) The impact of sample non-normality on ANOVA and alternative methods. Br J Math Stat Psychol 66(2):224–244
[28] Royston JP (1982) An extension of Shapiro and Wilk's W test for normality to large samples. J Roy Stat Soc: Ser C (Appl Stat) 31(2):115–124
[29] Conover WJ, Johnson ME, Johnson MM (1981) A comparative study of tests for homogeneity of variances, with applications to the outer continental shelf bidding data. Technometrics 23(4):351–361
[30] Dunn OJ (1964) Multiple comparisons using rank sums. Technometrics 6(3):241–252
[31] Burnham KP, Anderson DR (2014) P values are only an index to evidence: 20th-vs. 21st-century statistical science. Ecology 95(3):627–630
[32] Murtaugh PA (2014) In defense of P values. Ecology 95(3):611–617
[33] Charnes A et al (1997) Data envelopment analysis theory, methodology and applications. J Oper Res Soc 48(3):332–333
[34] Adler N, Friedman L, Sinuany-Stern Z (2002) Review of ranking methods in the data envelopment analysis context. Eur J Oper Res 140(2):249–265
[35] Todoroki C, Carson S (2003) Managing the future forest resource through designer trees. Int Trans Oper Res 10(5):449–460
[36] López-Espín JJ et al (2014) Benchmarking and data envelopment analysis An approach based on metaheuristics. Procedia Comput Sci 29:390–399
[37] Urbanik TJ (2001) Effect of corrugated flute shape on fibreboard edgewise crush strength and bending stiffness. J Pulp Pap Sci 27(10):330–335
[38] Clark RB, Cowey JB (1958) Factors controlling the change of shape of certain nemertean and turbellarian worms. J Exp Biol 35(4):731–748
[39] Goriely A, Tabor M (2013) Rotation, inversion and perversion in anisotropic elastic cylindrical tubes and membranes. Proc R Soc Math Phys Eng Sci 469(2153):20130011
[40] Horgan CO, Murphy JG (2018) Magic angles for fibrous incompressible elastic materials. Proc R Soc A Math Phys Eng Sci 474(2211):20170728
[41] Sharabi M et al (2018) Three-dimensional microstructural reconstruction of the ovine intervertebral disc using ultra-high field MRI. Spine J 18(11):2119–2127
[42] Qi N et al (2015) Investigation of the optimal collagen fibre orientation in human iliac arteries. J Mech Behav Biomed Mater 52:108–119
[43] Leelavanichkul S, Cherkaev A (2004) Why the grain in tree trunks spirals: a mechanical perspective. Struct Multidiscip Optim 28(2):127–135
[44] Demirkoparan H, Pence TJ (2015) Magic angles for fiber reinforcement in rubber-elastic tubes subject to pressure and swelling. Int J Non-linear Mech 68:87–95
[45] Lichtenegger H et al (1999) Variation of cellulose microfibril angles in softwoods and hardwoods—a possible strategy of mechanical optimization. J Struct Biol 128(3):257–269
[46] Donaldson L (2008) Microfibril angle: measurement, variation and relationships—a review. IAWA J 29(4):345–386
[47] Sorieul M et al (2016) Plant fibre: Molecular structure and biomechanical properties, of a complex living material, influencing its deconstruction towards a biobased composite. Materials 9(8):1–36
[48] Burgert I, Fratzl P (2009) Plants control the properties and actuation of their organs through the orientation of cellulose fibrils in their cell walls. Integr Comp Biol 49(1):69–79
[49] Xu P et al (2011) Mechanical performance and cellulose microfibrils in wood with high S2 microfibril angles. J Mater Sci 46(2):534–540. https://doi.org/10.1007/s10853-010-5000-8

[50] Coffin DW (2005) The creep response of paper. In: 13th fundamental research symposium: advances in paper science and technology. Lancashire, England, pp 651–747

[51] Lotfy M, El-osta M, Wellwood RW (1972) Short-term creep as related to microfibril angle. Wood Fiber 4(1):26–32

[52] Hunt DG (1986) The mechano-sorptive creep susceptibility of two softwoods and its relation to some other materials properties. J Mater Sci 21(6):2088–2096. https://doi.org/10.1007/BF00547951

[53] Bengtsson C (2001) Mechano-sorptive bending creep of timber - Influence of material parameters. Holz als Roh - und Werkstoff 59(4):229–236

[54] Gray-Stuart EM et al (2022) Influence of different box preparations on creep performance of corrugated fibreboard boxes subject to constant and cycling relative humidity environments. Packag Technol Sci

[55] Gajewski T et al (2021) Crushing of double-walled corrugated board and its influence on the load capacity of various boxes. Energies 14(14):4321

[56] Garbowski T et al (2021) Crushing of single-walled corrugated board during converting: experimental and numerical study. Energies 14:3203

[57] Nevins AL (2008) Significant factors affecting horticultural corrugated fibreboard strength: a thesis presented in partial fulfilment of the requirements for the degree of Doctor of Philosophy in Food Engineering at Massey University, Palmerston North, New Zealand. Massey University.